
When Probing Accuracy Saturates, Fragility Resolves: A Complementary Metric for LLM Pre-Training Analysis

Orion Reblitz-Richardson*

Abstract

Standard linear probing declares a property “encoded” when a classifier on hidden states achieves high accuracy. The protocol works well on a snapshot but breaks across pre-training: probe accuracy saturates within the first few thousand steps, leaving most of training invisible to the instrument.

We introduce *fragility*, a complementary per-layer metric defined as the activation-noise level at which probe accuracy collapses. Fragility is sensitive to both the margin of separability and the redundancy of representation, both of which keep evolving long after accuracy plateaus.

Applied to open-checkpoint language models, fragility recovers structure that accuracy alone cannot see. Moralized representations emerge along a *lexical* \rightarrow *compositional gradient*: lexical moral detection first, compositional moral encoding later. Because probe accuracy on its own tracks how lexically separable a dataset is, we establish the compositional encoding directly, by showing it transfers across construction types that share no contrast tokens. A *layer-depth robustness gradient* develops monotonically across training while accuracy stays flat. And matched fine-tuning corpora that produce identical probing accuracy leave distinct fragility fingerprints, showing that data curation reshapes probe robustness without changing probe accuracy.

In every comparison we test, where probing accuracy returns a flat answer, fragility returns a structured one.

1 Introduction

A standard interpretability protocol works as follows: given a representation of interest from a large language model, train a linear classifier to predict the property from frozen hidden states, report classifier accuracy at each layer, and declare the property “linearly encoded” wherever accuracy is high. The protocol is well-established (Alain and Bengio, 2017, Belinkov, 2022) and works well for asking *whether* a model represents a property at a given snapshot.

It does not work well for asking *how a representation evolves during pre-training*. We demonstrate the failure mode concretely. On the OLMo-2 1B early-training trajectory (Groeneveld et al., 2024), 37 model checkpoints densely sampled at 1K-step intervals across steps 0-36K (~76B tokens), a binary linear probe trained on a 240-pair moral / neutral minimal-pair dataset reaches ~95% mean accuracy across all 16 transformer layers by step 4K. For the remaining ~33K training steps (~95% of the trajectory we have data for), the standard probing instrument returns essentially the same number; whatever continued representational change the model undergoes through that period is invisible to it.

This paper makes a methodological contribution that takes the saturation problem as a fixed feature of probing accuracy and adds a complementary metric to recover the missing resolution: *fragility*,

*Distiller Labs. Correspondence to Distiller Labs <orion@orionr.com>.

defined as the activation-noise level at which probe accuracy drops below a threshold. Formally, for layer ℓ with trained probe f_ℓ , standard probing reports test-set accuracy $A(f_\ell)$. We define the **critical noise** σ_ℓ^* as the smallest noise scale at which accuracy under Gaussian perturbation drops below a fragility threshold τ :

$$\sigma_\ell^* = \min \{ \sigma \in \mathcal{S} : A(f_\ell, h_\ell + \varepsilon) < \tau, \quad \varepsilon \sim \mathcal{N}(0, \sigma^2 I) \}$$

where $\mathcal{S} = \{0.1, 0.3, 1.0, 3.0, 10.0\}$ and $\tau = 0.6$ (if no σ in \mathcal{S} brings accuracy below τ , $\sigma_\ell^* = \max(\mathcal{S}) = 10.0$). A low σ_ℓ^* means the representation at layer ℓ is **fragile**: probe accuracy collapses under small noise. A high σ_ℓ^* means the encoding is **robust**: the distinction is encoded with wide margin and/or redundancy. Fragility is a per-layer measurement applied to the same trained probe used for the accuracy curve, and it is sensitive to both the *margin* of separability and the *redundancy* of representation, both of which keep evolving through training even after accuracy has plateaued (it does not separately identify their contributions; see Section 5.2). We use fragility to map structural representational change that probing accuracy alone cannot see, and to establish three findings on the OLMo-2 1B and OLMo-3 7B open-checkpoint family that together earn the methodological claim its keep:

Finding 1: Moralized semantic distinctions emerge along a quantitative lexical→compositional gradient. A standard moral probe (single morally-loaded lexeme swap) onsets at step 1K. A *compositional* moral probe (pairs that hold the action verb constant and vary only individually-mild tokens whose moral status flips in context (“protect” / “humiliate”, “hungry” / “wealthy”, “innocent” / “guilty”)) onsets at step 5K under 4-seed averaging (per-seed range 4K-7K), between sentiment (2K) and syntax (6K). The standard probe’s step-1K onset measures how quickly moralized vocabulary becomes linearly separable, not how quickly moral valence is encoded compositionally; the gradient reading is the honest one.

Finding 2: A layer-depth robustness gradient develops monotonically over training, invisible to probing accuracy. Mean accuracy plateaus by step 4K but mean critical noise continues to evolve through step 36K: late layers hold maximum robustness while early-layer critical noise drops from 10.0 to 1.8 between steps 4K and 36K. The pattern reproduces at the OLMo-3 7B scale with steeper late-layer dominance, and reproduces independently for the compositional probe across four random-seed splits.

Finding 3: Data curation reshapes probe robustness without changing probe accuracy. LoRA fine-tuning on three matched corpora (narrative- moral, declarative-moral, general non-moral control) produces identical probing accuracy across conditions (final peak 0.740 / 0.750 / 0.750) but distinct fragility profiles. Declarative moral training (“Stealing is wrong” repeated) produces fragility dips at 10 of 16 layers (mean critical noise 5.63) versus 6-7 fragile layers for natural-text conditions (mean 6.94 / 7.38). Accuracy says “no signal”; fragility says “declarative training creates broadly fragile representations.”

All experiments run on a single MacBook Pro M4 Pro with MPS; ~6 hours total MPS time. Code, datasets (including the 200-pair compositional moral minimal-pair dataset that is itself a methodological contribution), per-checkpoint outputs, and 4-seed fragility replications are released with the paper.

The unifying claim is methodological, not moral-domain-specific: **in every comparison we test, where probing accuracy returns a flat answer, fragility returns a structured one.** Section 2 places the work against related literatures; Section 3 details the four minimal-pair datasets, linear probing, and the fragility test; Section 4 reports results; Section 5 discusses the phase-transition-vs-gradual-emergence taxonomy implied by Finding 1, the geometric reasons fragility succeeds where accuracy saturates, and limitations; Section 6 concludes.

2 Related work

Linear probing. [Alain and Bengio \(2017\)](#) established linear probing as a layer-wise diagnostic for what intermediate representations contain; [Belinkov \(2022\)](#) surveys the methodology’s promise and known limitations. Subsequent work has formalized accuracy-based probing’s structural shortcomings via control tasks ([Hewitt and Liang, 2019](#)), information-theoretic probing ([Pimentel et al., 2020](#)), and minimum-description-length analyses ([Voita and Titov, 2020](#)). Our methodological contribution

extends the saturation concern: where the probing literature treats ceiling effects as a threat to validity, we treat them as a fixed feature of the instrument and add a complementary metric (fragility) that continues to resolve representational change after accuracy plateaus.

Activation perturbation. [Borras et al. \(2022\)](#) proposed “Walking Noise,” injecting additive Gaussian noise at individual layers and defining a per-layer midpoint noise level, the closest prior concept to our per-layer critical noise. However, Walking Noise measures end-to-end *task accuracy* degradation, not probe accuracy on specific concepts, and evaluates a single trained model rather than tracking across training checkpoints. APEX ([Ren et al., 2026](#)) injects Gaussian noise into hidden activations and defines “escape noise” (the noise scale at which output becomes independent of input), analogous to our critical noise; but APEX measures model-output distribution changes, not concept-specific probe accuracy. Our method combines per-layer noise robustness with concept-specific probing *across* training checkpoints, a combination that neither approach attempts.

Probing across training. [Qian et al. \(2024\)](#) applied linear probes to 360 pre-training checkpoints (LLM360 Amber 7B) for five trustworthiness dimensions, observing a fitting-and-compression pattern. Their work establishes the “probing across checkpoints” approach but tracks only probe *accuracy*, which is exactly what we show saturates early and stops returning information. Our fragility metric recovers the dynamics that continue after the point where their approach loses resolution.

Causal tracing. [Meng et al. \(2022\)](#) introduced ROME and the causal-tracing methodology, which distinguishes layers that *encode* information from layers that *causally use* it. Our 7B causal-probing analysis (Appendix B) finds a ~10-layer divergence between probing peak and causal peak for moral information, replicating the storage-vs-use distinction in the moral domain as supporting evidence for the body’s methodological thesis.

Phase transitions. [Power et al. \(2022\)](#) documented “grokking,” sudden phase transitions from memorization to generalization, with subsequent mechanistic work attributing such transitions to discrete circuit formation ([Nanda et al., 2023](#), [Olsson et al., 2022](#)). Our Section 4.1 finding that semantic minimal-pair tasks (standard moral, sentiment) emerge as sharp phase transitions while compositional and structural tasks emerge gradually maps the grokking phenomenon against a lexical-vs-compositional dichotomy *within a single training run*, to our knowledge a novel framing.

Moral Foundations Theory. The standard moral dataset organizes content across [Haidt’s \(2012\)](#) and [Graham et al.’s \(2013\)](#) six MFT foundations (care/harm, fairness/cheating, loyalty/betrayal, authority/subversion, sanctity/degradation, liberty/oppression). MFT is used as a *construction* heuristic for balanced coverage, not as a cognitive claim about how language models represent morality. The compositional dataset (Section 3.2) categorizes by construction pattern (motive / target / consequence / role) instead.

OLMo. [Groeneveld et al. \(2024\)](#) released the OLMo family with full intermediate checkpoint releases (the infrastructure that makes dense-sampling trajectory analysis possible), extended in the OLMo-2 release ([OLMo Team, 2025](#)) to substantially longer training schedules. Our 37-checkpoint 1B early-training and 20-checkpoint 7B stage-1 trajectories rely on these open releases; the methodology applies to any open-checkpoint family with dense enough sampling. Pythia ([Biderman et al., 2023](#)) offers a complementary open-checkpoint testbed.

Single-direction circuits. [Arditi et al. \(2024\)](#) demonstrated refusal behavior in instruction-tuned models is mediated by a single representational direction. The fragility metric is the pre-training-time analog: where single-direction-refusal asks whether *post-training* safety properties are concentrated in narrow circuits at the final checkpoint, we ask whether moralized representations pass through more or less brittle states *during* training. Both literatures address how concentrated vs. distributed safety-relevant representations are, at different points in the model lifecycle. Representation-engineering more broadly ([Zou et al., 2023](#)) treats interpretability as direct readout of learned representations.

Scope. We use moralized vocabulary as a demonstration domain. The compositional probe (Section 3.2) is the explicit lexical- accessibility ablation; deeper questions (counterfactual moral reasoning, generalization to held-out moral structures) would require harder probes and are discussed as future work in Section 5.3.

3 Methodology

We apply linear probing classifiers on four matched minimal-pair datasets to all 37 OLMo-2 1B early-training checkpoints, 20 OLMo-3 7B stage-1 checkpoints, and the OLMo-2 1B final checkpoint. Two probe families: LayerWiseMoralProbe (per-layer accuracy) and MoralFragilityTest (per-layer noise robustness). All experiments run on a single MacBook Pro M4 Pro / MPS; code, datasets, and per-checkpoint outputs are released with the paper.

3.1 Standard minimal-pair datasets

Three single-token-swap datasets mirror established minimal-pair probing practice (Belinkov, 2022) by holding the syntactic skeleton constant and swapping a single token: **moral / neutral** (240 pairs, 40 per Moral Foundations Theory category (care/harm, fairness/cheating, loyalty/betrayal, authority/subversion, sanctity/degradation, liberty/oppression; Haidt, 2012; Graham et al., 2013; e.g. “She betrayed the woman” / “She greeted the woman”). The moral pairs are drawn from a 1,200-pair dataset constructed per published quality guidelines with LLM-assisted filtering for naturalness and moral neutrality of neutral-side sentences (see DATASET_GUIDELINES.md); 240 pairs (40 per foundation) are subsampled with a deterministic seed. **Sentiment** (210 pairs across ten domains; positive / negative adjective swap, e.g. “... excellent food...” / “... terrible food...”); **syntax** (210 pairs targeting local grammaticality violations (word-order swaps, agreement, auxiliary misplacement), e.g. “She handed the finished report...” / “She handed finished the report...”). All three use a length-ratio gate ≤ 1.5 and a deterministic seed-42 train / test split. They establish the baseline emergence ordering in Section 4.1.

3.2 Compositional moral probing dataset

The standard moral probe’s pairs differ in a single morally-loaded lexeme, which a linear probe can separate from single-token distributional statistics alone. The standard probe’s step-1K onset therefore measures *how quickly moralized vocabulary becomes linearly separable from neutral vocabulary*, not *how quickly moral valence is encoded compositionally*. To bound this lexical-accessibility framing empirically, we construct a compositional moral minimal-pair dataset whose pairs require multi-word integration to determine moral valence. This dataset is a primary methodological contribution of the paper.

Construction. Each pair holds the action verb constant and varies 1–2 individually-mild tokens whose moral status only resolves in the surrounding action context. Four 50-pair categories (200 pairs total), all hand-curated:

- *action_motive*: same action verb, motive determines valence. “She lied to her parents to **protect** her younger brother today” / “... to **humiliate**...”
- *action_target*: same action, target descriptor determines moral relevance. “He gave the last loaf of bread to the **hungry** stranger at the door” / “... the **wealthy** stranger...”
- *action_consequence*: same action, consequence framing determines valence. “He kept the secret about the surprise to keep his sister **safe** today” / “... to keep his sister **hurt** today”
- *role_reversal*: same components, role / target / context determines valence. “The judge accepted the gift to free the **innocent** prisoner from prison” / “... the **guilty** prisoner...”

Contrast tokens are individually mild: protect, humiliate, hungry, wealthy, safe, hidden, innocent, guilty. None appear in the strong-valence blocklist of 47 tokens (murder, torture, stole, rape, assault, etc.) we use as a construction gate. Each token is unmarked or only weakly valenced in isolation; the moral signal in each pair lives in the integration of the contrast token with the surrounding action context.

Validation gates. All 200 pairs pass five gates simultaneously (validate_compositional_dataset):

1. *Length difference*: per-pair absolute difference ≤ 2 alphabetic tokens.
2. *Length band*: both halves in the 8-20-word band.
3. *Content-word overlap*: per-pair ≥ 0.60 with stopwords removed (|shared| / max(|moral|, |immoral|)). This metric matches deepsteer.datasets.

`validation.validate_pairs` so the 0.60 threshold here is directly comparable to the standard moral probe gate.

4. *Strong-valence blacklist*: zero tokens from the 47-word blacklist on either side.
5. *No exact duplicates* of either side across the 200 pairs.

Operationalizing “compositional”: transfer and lift, not a bag-of-words gate. A minimal pair that flips its label by swapping a single contrast token makes that token a lexical cue *by construction*: a bag-of-words classifier separates the seen pairs no matter how mild the token is in isolation. “Can unigrams separate the data” is therefore the wrong question (they can: a pair-disjoint, orientation-invariant unigram TF-IDF classifier reaches 0.63 overall and 0.57-0.64 per construction, where pair-disjoint means `GroupKFold` keyed on pair so neither half of a pair leaks across the split, and orientation-invariant means scoring $\max(\text{acc}, 1 - \text{acc})$). The right question is whether the hidden-state representation encodes moral valence in a way that generalizes *beyond the specific contrast tokens*. We operationalize compositional encoding through two tests, both measured against this unigram TF-IDF baseline (the *lexical floor*):

1. *Leave-construction-out transfer*. Train the probe on three of the four construction categories and test on the held-out fourth, which shares almost no contrast tokens with the training categories. A probe relying on token identity cannot transfer; a construction-general representation can.
2. *Lift over the lexical floor*. Within each construction, compare hidden-state decodability (pair-disjoint CV) to that construction’s unigram lexical floor. The gap is signal the bag-of-words baseline cannot reach.

Section 4.1 reports both, at the final checkpoint and across training. (The construction iterated through ~5 rewriting passes to satisfy the 0.60 content-overlap gate alongside the multi-word contrast requirement; the two constraints are in genuine tension; see Appendix D.)

Train / test split. 160 / 40, stratified by category (40 train + 10 test per category), seed = 42. The dataset and validation gates are deterministic, API-free, and included in the toolkit at `deepsteer/datasets/compositional_moral_pairs.py`.

3.3 Linear probing

Identical probing methodology across all four datasets: when we report a 4K-step gap between standard and compositional moral onsets (Section 4.1), the only experimental variable is the dataset.

For each transformer layer ℓ we mean-pool hidden states across the sequence dimension and train a binary linear classifier (`nn.Linear(hidden_dim, 1)`) to distinguish the two sides of each minimal pair, with BCE-with-logits loss, Adam ($\text{lr} = 1\text{e-}2$), 50 epochs, no weight decay or early stopping; probes run in fp32 on fp16 activation caches collected via PyTorch forward hooks on the `HuggingFace model.layers[l]` modules. We report per-layer test-set accuracy and four summary statistics: onset layer (first ≥ 0.6), peak layer, encoding depth (`onset_layer / n_layers`), and encoding breadth (fraction of layers ≥ 0.6). The compositional probe additionally tracks a TF-IDF content-only floor per checkpoint that hidden-state probing must beat by ≥ 10 pp. Implementation: `LayerWiseMoralProbe` for standard and compositional moral (the latter a subclass that overrides only the dataset path), `GeneralLinearProbe` for sentiment and syntax (same training loop).

3.4 Fragility testing

Train per-layer linear probes on clean activations as in Section 3.3; for each layer ℓ , add Gaussian noise $N(0, \sigma^2)$ to the cached test-set activations and re-evaluate the trained probe across a logarithmic sweep $\sigma \in \{0.1, 0.3, 1.0, 3.0, 10.0\}$. The smallest σ at which accuracy drops below the fragility threshold (0.6, i.e. chance + 0.1 on a binary task) is the layer’s *critical noise*; if no σ in the sweep brings the probe below threshold, critical noise is reported as the maximum (10.0). Per-layer critical noise gives the fragility profile; its mean is `mean_critical_noise` as a scalar summary. The same `MoralFragilityTest` runs against both the standard and compositional datasets; methodology generality is established by reuse, not reimplemention.

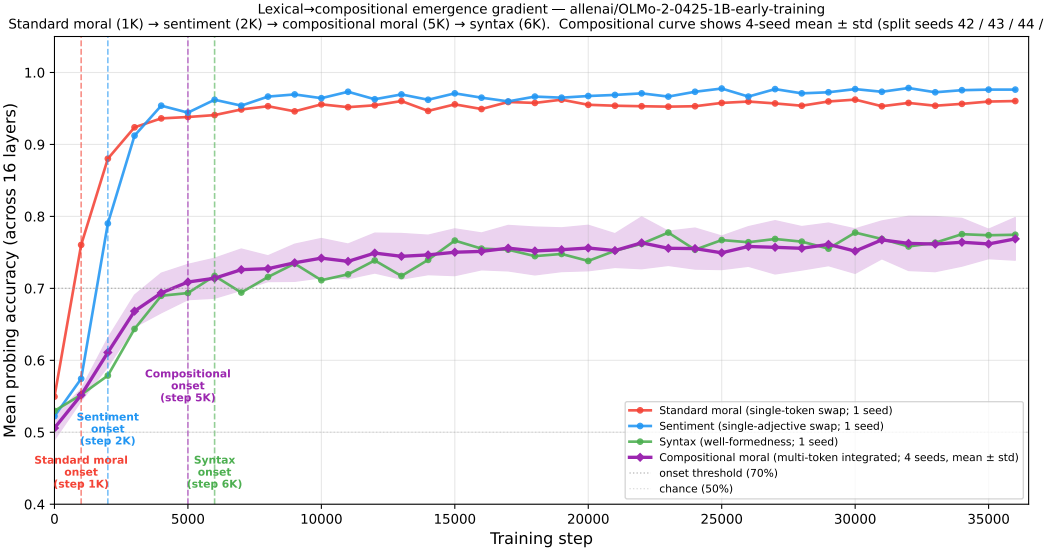


Figure 1: Lexical \rightarrow compositional emergence gradient on OLMo-2 1B early-training. Standard moral and sentiment probes (single-token swap) plateau near 0.97; compositional moral and syntax (multi-token integration) plateau near 0.77. Compositional curve is 4-seed mean \pm std (split seeds 42/43/44/45). Onsets: standard moral 1K, sentiment 2K, compositional moral 5K (per-seed range 4K–7K), syntax 6K.

3.5 Target models and checkpoints

Three OLMo (Groeneveld et al., 2024, OLMo Team, 2025) base models. **OLMo-2 1B early-training** (allenai/OLMo-2-0425-1B-early-training), 37 checkpoints at 1K-step intervals from step 0 to step 36K (\sim 76B tokens), the primary data source for Section 4.1 onsets and Section 4.2 fragility. **OLMo-3 7B stage 1** (allenai/OLMo-3-7B), 20 checkpoints through \sim 1.4M steps (\sim 10T tokens), Section 4.2 7B corroboration and Appendix B causal tracing. **OLMo-2 1B final** (allenai/OLMo-2-0425-1B, \sim 2.2T tokens), used only for the compositional probe validation gate (Section 3.2). All loaded in fp16 on MPS; \sim 6 hours of MPS time across the full Section 4 experimental record.

3.6 Validity controls

Three controls standard for linear-probing studies (leave-lexeme-out splits, paraphrase transfer, adversarial lexical swap) are reported in Appendix C. The compositional probe (Section 3.2) addresses the strongest version of “your probe is just reading vocabulary”: its compositional encoding is established by leave-construction-out transfer and lift over the unigram lexical floor (Section 3.2, Section 4.1), not by the lexical floor alone, and it is a strictly stronger ablation than those three controls combined for the relevant question.

4 Results

4.1 Emergence ordering: a lexical \rightarrow compositional gradient

We train the four linear probes from Section 3.1–Section 3.2 on hidden states from all 37 OLMo-2 1B early-training checkpoints (steps 0–36K at 1K intervals). Onset is the first checkpoint where mean probe accuracy across all 16 layers reaches 0.70.

Figure 1 plots the four mean-accuracy trajectories on a shared step axis.

Probe	Construction	Onset step	Onset mean acc	Plateau mean acc (step 36K)
Standard moral	single morally-loaded lexeme swap	1,000	0.760	0.960
Sentiment	single valenced adjective swap	2,000	0.790	0.976
Compositional moral	multi-token integrated swap	5,000	0.709 ± 0.025	0.769 ± 0.030
Syntax	structural well-formedness	6,000	0.717	0.774

Table 1: Probe onset and plateau by construction. Compositional moral values are 4-seed mean \pm std (split seeds 42 / 43 / 44 / 45). Per-seed compositional onsets: 4K, 4K, 7K, 7K (substantial seed variance, with the 4-seed mean curve crossing 0.70 at step 5K). The single-seed standard moral / sentiment / syntax curves are reported without std bands; their seed dependence is not characterized.

(1) The four probes resolve into a quantitative lexical \rightarrow compositional gradient. The standard moral probe (single morally-loaded lexeme swap, “betrayed” / “greeted”) onsets at step 1K. The compositional moral probe (multi-token integrated swap; contrast tokens “protect” / “humiliate”, “hungry” / “wealthy” are individually mild) onsets at step 5K under 4-seed averaging, a 4K-step lag, with per-seed onsets ranging 4K-7K and overall trajectory always between sentiment (2K) and syntax (6K). The standard probe’s step-1K onset measures how quickly moralized vocabulary becomes linearly separable, not how quickly moral valence is encoded compositionally. Both findings are true; the strongest single-token reading of the standard onset is ruled out, while the gradient reading (lexically-marked moralized vocabulary first, compositional moral integration second, syntactic competence last) holds. Onset accuracy alone understates the case: the 0.709 onset sits only \sim 8 pp above the 0.63 lexical floor, and onset ordering across all four datasets tracks lexical-floor height (unigram TF-IDF floor: standard moral 0.86, sentiment 0.80, compositional 0.63, syntax 0.59; the more lexically separable a dataset, the earlier its onset and the higher its plateau). Onset timing on its own therefore does not separate compositional encoding from lexical difficulty. The evidence that the probe recovers compositional rather than lexical signal comes from transfer and lift (Section 3.2).

(1b) Compositional encoding is real, not lexical lookup (final-checkpoint evidence). At the OLMo-2 1B final checkpoint (\sim 2.2T tokens), a probe trained on three construction categories and tested on the held-out fourth transfers at **0.848** mean (0.80-0.91 across the four held-out constructions), essentially matching its in-distribution pair-disjoint accuracy (**0.858** @ layer 7), while a bag-of-words classifier doing the same leave-construction-out transfer collapses to **0.598**. Within each construction the probe decodes +0.20 to +0.28 above the unigram lexical floor. The decisive case is *role_reversal*, where the same components appear on both sides and the lexical floor is lowest (0.57): hidden states still decode moral valence at 0.85 (lift +0.28) and held-out transfer reaches 0.81. A probe reading contrast-token identity could not do this; the model reads moral valence from context. This is the operational content of “compositional” in this paper, and it is a positive result, not a thin margin over a bag-of-words floor.

(1c) Compositional encoding emerges in early pre-training, then holds.

Figure 2 plots the transfer-and-lift analysis across all 37 early-training checkpoints. At initialization the encoding is absent: leave-construction-out transfer sits at chance (0.55) and lift is \sim 0. It emerges over steps 2K-9K, crossing the bag-of-words transfer floor (\sim 0.60) by step 2K (0.667), passing 0.70 by step 3K, reaching 0.78 by step 5K, then plateauing by step \sim 9K at transfer \sim 0.82 and lift \sim +0.20 and holding there through step 36K (0.83 / +0.22). The *role_reversal* construction, where lexical cues are scrambled by design, follows the same curve (panel a). The encoding also localizes in depth: once it appears, the most decodable layer settles into mid-network (layers 8-10) and stays there for the rest of the trajectory (panel b). Compositional moral encoding is therefore an early-pre-training acquisition, emerging after lexical moral detection (standard-probe onset at step 1K) and consistent with the lexical \rightarrow compositional ordering, that once acquired is stable across the remaining \sim 30K steps we observe. Numbers source: outputs/phase_c4_compositional/b_traj/ (per-checkpoint) and b_traj_summary.json.

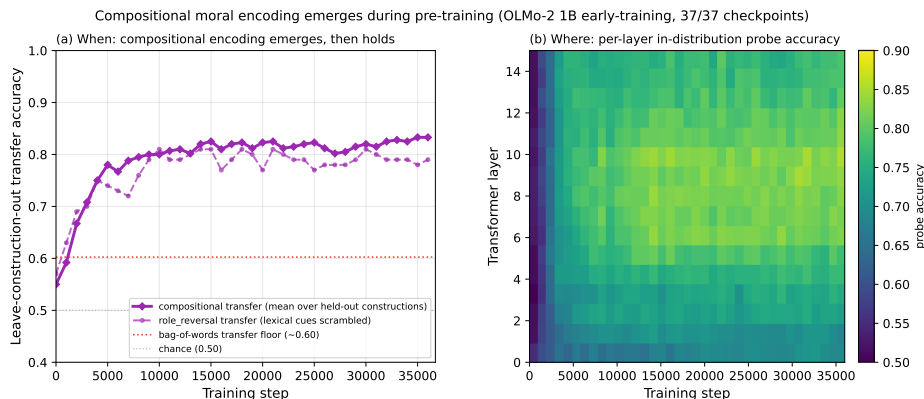


Figure 2: Compositional moral encoding emerges in early pre-training and then holds (OLMo-2 1B early-training, 37 checkpoints). (a) When: leave-construction-out transfer accuracy rises from chance (~ 0.55) across steps 2K–9K, crosses the bag-of-words transfer floor (~ 0.60) by step 2K, and plateaus near 0.82 (lift $\sim +0.20$ over the lexical floor) through step 36K; the role_reversal curve (lexical cues scrambled) tracks it. (b) Where: per-layer in-distribution probe accuracy, showing the encoding concentrating in mid-network layers 8–10 once it emerges.

(2) Step-like vs. gradual emergence dichotomy. Standard moral and sentiment probes show sharp sigmoidal transitions (chance \rightarrow plateau within one 1K-step interval at onset, then flat). Compositional moral and syntax rise more gradually (~ 3 -5K steps across the 0.70 threshold). At 1K sampling we resolve transitions that are step-like at this resolution; we do not claim true discontinuity. This parallels grokking-literature observations (Power et al., 2022) that some capabilities emerge sharply and others gradually; the within-run split here suggests the distinguishing factor is whether the capability is acquirable from local lexical statistics (sharp) or requires multi-token integration (gradual). Section 5.1 develops.

(3) Plateau coincidence. The four-curve overlay (Figure 1) makes a structural caveat visually inescapable: probes whose signal lives in single-token vocabulary statistics (standard moral, sentiment) plateau at 0.96 and 0.98, while probes whose signal requires multi-token structural or compositional integration (compositional moral, syntax) plateau at 0.77 and 0.77. The 20-percentage-point ceiling gap is consistent across the entire 0-36K trajectory. This may be a probe-side property under our methodology rather than a model property: either the 1B model encodes both compositional moral valence and syntactic well-formedness at ≈ 0.77 (model ceiling), or mean-pooled linear probing on 1B hidden states bottoms out at ≈ 0.77 for multi-token integration regardless of underlying representational quality (probe ceiling). The cleanest disambiguation is repeating Section 4.1 at 7B and 32B: if compositional moral rises with scale while syntax does not, the model is the bottleneck; otherwise the probe is. We state both readings honestly in Section 5.3 and refine rather than overturn the gradient finding.

Generalization to OLMo-3 7B. We have not yet run the compositional probe on the OLMo-3 7B trajectory; doing so is the cleanest disambiguation of the plateau-coincidence ambiguity and is flagged as future work in Section 5.3.

Numbers source: `outputs/phase_c2/c2_emergence_timing.json` (standard moral + sentiment + syntax, 37 checkpoints) and `outputs/phase_c4_compositional/c4_emergence_timing.json` (compositional moral, 37 checkpoints; companion JSON with all four curves overlaid). Validation source: `outputs/phase_c4_compositional/c4_validation.json` (final-checkpoint validation gate on `allenai/OLMo-2-0425-1B`).

4.2 Probing accuracy saturates; fragility doesn't

Figure 3 provides the central comparison for the methodological claim: a two-panel comparison on a shared step axis. Top panel: mean probing accuracy, a sharp sigmoid from chance (~ 0.59) to a plateau (~ 0.95) between steps 0 and 4K, then flat for the remaining ~ 33 K steps. Bottom panel: mean fragility, an initial rise alongside accuracy in the first few thousand steps, then continued movement throughout.

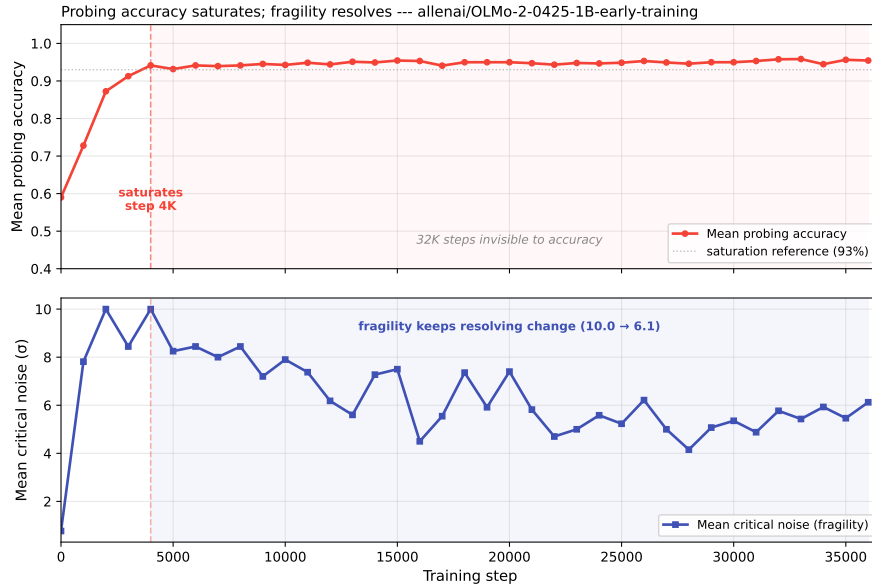


Figure 3: Probing accuracy saturates; fragility resolves. OLMo-2 1B early-training, 37 checkpoints. Top: mean probing accuracy across all 16 layers — saturates near 0.95 by step 4K and stays flat for the remaining 32K steps. Bottom: mean critical noise — continues evolving long after accuracy plateaus, drifting from ~ 10 down toward ~ 6 between steps 4K and 36K.

Top panel reaches a ceiling and stops; bottom panel keeps moving for the entire remaining 90 % of training.

OLMo-2 1B, 37 checkpoints, dense sampling.

Step	Mean acc	Mean critical noise	Late-layer crit	Mid-layer crit	Early-layer crit
0	0.590	0.77	0.1	0.6	1.6
1,000	0.728	7.81	10.0	8.8	4.4
4,000	0.941	10.0	10.0	10.0	10.0
10,000	0.943	7.90	10.0	8.8	7.2
15,000	0.954	7.50	10.0	10.0	5.0
20,000	0.950	7.40	10.0	10.0	2.2
36,000	0.954	6.12	10.0	6.5	1.8

Table 2: Standard moral probe. Accuracy plateaus by step 4K; fragility evolves through step 36K with a layer-depth gradient that develops monotonically (late > mid > early after step $\sim 15K$).

Figure 4 shows the same trajectory as two stacked layer-depth heatmaps: probing accuracy (uniformly green after step 4K, no remaining structure to resolve) above critical noise (gradient emerging: late layers hold maximum noise tolerance throughout while early layers grow progressively more brittle). Same data; different metric; different visible structure.

The pattern reproduces at OLMo-3 7B (5 sparse checkpoints): mean critical noise rises $2.68 \rightarrow 5.14$ between steps 0 and 353K, then holds at ~ 5.3 through step 1.4M; layer-depth gradient is steeper (late ~ 10.0 / mid ~ 6.2 / early ~ 2.0) and the most-robust layer drifts deeper across training (layer 1 $\rightarrow 15 \rightarrow 16 \rightarrow 10 \rightarrow 10$). The 1B trajectory is the headline because dense 1K-step sampling resolves the saturation step ($\sim 4K$) and gradient emergence rate.

Compositional probe fragility evolution (4-seed replication; the methodological claim generalizes beyond the standard probe). We ran `MoralFragilityTest` (Section 3.4) on the compositional dataset across all 37 OLMo-2 1B early-training checkpoints with four split seeds (42, 43, 44, 45), the original seed-42 trajectory plus a three-seed replication ~ 50 min on the same MacBook Pro M4 Pro / MPS. **Table 3** gives the 4-seed mean \pm std at the diagnostic checkpoints; the 4-seed accuracy band on **Figure 1** carries the matching probing- side trajectory.

Step	Compositional mean critical noise (4-seed mean \pm std)	n
------	---	---

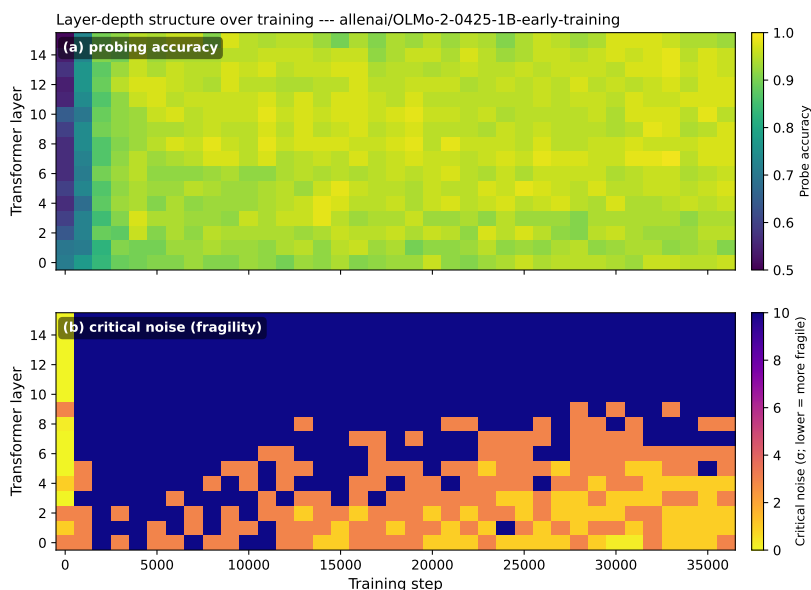


Figure 4: Layer-depth structure over training (OLMo-2 1B early-training). (a) Probing accuracy: uniformly high across layers after step 4K. (b) Critical noise: a layer-depth gradient develops, with late layers holding maximum noise tolerance while early layers grow progressively more brittle. Same data, same model; structure visible only under the fragility metric.

if 4-seed mean critical noise drops by ≥ 1.0 between step 7K and step 30K *and* seed-to-seed std at both endpoints is smaller than the gap. Realized values: gap = $4.65 - 2.46 = 2.19$ (≥ 1.0 \checkmark), max endpoint std = 0.84 (< 2.19 \checkmark). Both pass with substantial margin; the post-step-7K decline is a stable property across the four split seeds.

Two non-exclusive readings of the diverging long-term direction (7B / 32B replication disambiguates both): a *mechanism reading* (as training continues on text that does not specifically reinforce compositional moral integration, the compositional representation drifts toward brittleness while standard-probe representations are continually reinforced by moralized vocabulary density) and a *probe-ceiling reading* (fragility at the 0.77 operating point has less headroom than at 0.96, partly artifacting the difference). We state both in Section 5.3 without commitment.

Numbers sources: outputs/phase_c1/RESULTS.md (1B standard probe), outputs/phase_b/ (7B corroboration), outputs/phase_c4_compositional/3seed/{aggregate_per_checkpoint, decision}.json (4-seed mean \pm std and decision rule application), outputs/phase_c4_compositional/3seed/4seed_fragility_evolution.png (headline 4-seed plot).

4.3 Data curation reshapes probe robustness, not probe accuracy

LoRA (Hu et al., 2022) fine-tuning on three matched corpora from the OLMo-2 1B step-1000 checkpoint (mid-transition, $\sim 80\%$ peak probing accuracy). Corpora: a 247K-token narrative-moral corpus (Aesop / Grimm / Andersen), a 500K-token declarative-moral corpus (template-expanded MORAL_SEEDS: “Stealing is wrong”), and a 420K-token general non-moral control (Darwin). Identical LoRA hyperparameters (rank 16, alpha 32, q_proj + v_proj, lr $2e-4$, batch 2, seq 1024, 1000 steps); standard moral probe + fragility every 100 LoRA steps.

Probing accuracy is identical across conditions. Final peak accuracy at LoRA step 1000: narrative 0.740, declarative 0.750, general control 0.750, all within 1 pp across very different training data. The accuracy metric returns no signal for which corpus produces what kind of representational change.

Fragility profiles are condition-specific (the main result). Final mean critical noise: narrative 7.38, declarative 5.63, general control 6.94. The per-layer breakdown separates the conditions: narrative

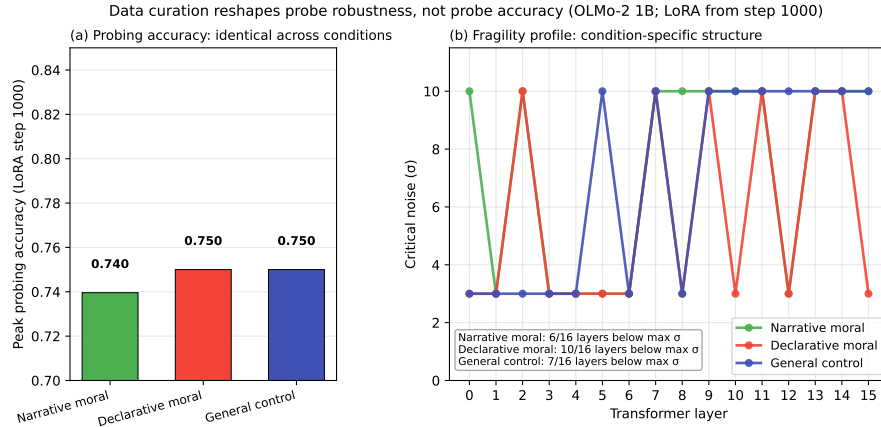


Figure 5: Data curation reshapes probe robustness, not probe accuracy (OLMo-2 1B; LoRA fine-tuning from step 1000 on three matched corpora). (a) Final probing accuracy is near-identical across narrative-moral, declarative-moral, and general-text control conditions (0.740 / 0.750 / 0.750). (b) Per-layer critical noise is condition-specific: declarative-moral training produces diffuse fragility across 10 of 16 layers (mean $\sigma^* = 5.63$ vs. 7.38/6.94 for natural-text conditions).

and general control show fragility dips at 6 and 7 of 16 layers respectively; the declarative condition shows dips at **10 of 16 layers**, creating a broadly more fragile representation than either natural-text condition.

Figure 5 plots all three per-layer profiles plus the three identical accuracy bars: same accuracy, different fragility.

Training loss is decoupled from representational change. Declarative loss drops 5.5 \rightarrow 1.0 (template memorization), narrative 4.3 \rightarrow 4.0, control 5.0 \rightarrow 4.4. The condition with the deepest loss reduction is the same condition with the most diffuse fragility; the two with the shallowest loss reductions retain more robust representations. The model is learning declarative templates as surface text patterns without that learning translating into either accuracy gains or robust representational structure.

Why diffuse fragility under declarative training? The declarative corpus consists of repeated syntactic templates (“X is wrong”, “Y is immoral”) that the model memorizes easily (loss \rightarrow 1.0). This memorization creates narrow pattern-matching features across multiple layers, features whose probe accuracy is maintained by low-margin decision boundaries that collapse under small noise. Narrative and general-control conditions produce fewer fragile layers because natural text has no repeated syntactic template; moral content in Aesop’s fables is embedded in diverse narrative structures, forcing the probe to rely on distributed features that tolerate noise. The declarative fragility pattern is consistent with the Section 4.2 finding that early layers grow progressively more brittle over training; declarative LoRA produces a diffuse version of a vulnerability pattern that pre-training produces as a layer-depth gradient.

This is direct evidence for the methodological thesis in a controlled setting: same data, same probe; accuracy returns no signal, fragility separates the conditions.

Why the fragility is diffuse rather than localized. The diffuse pattern, fragility across 10 of 16 layers (mean $\sigma^* = 5.63$ vs. 7.38 / 6.94) rather than a single dramatic dip, has a straightforward mechanistic explanation. When the probing dataset controls for animacy and register confounds (Section 3.1), the probe detects actual moral features at every layer rather than exploiting shortcuts like “is this about a person or a circuit?” that survive Gaussian perturbation easily. When declarative templates are memorized, the model’s moral representations throughout the network become template-dependent: narrow-margin features that collapse under noise at multiple layers rather than just one. Template memorization does not corrupt one layer; it degrades the network’s moral representations broadly. This sensitivity to dataset quality confirms the importance of the validation methodology described in Section 3.1: probing datasets that contain animacy or register shortcuts will systematically underestimate fragility at layers where the probe exploits those shortcuts rather than moral content.

Numbers source: `outputs/phase_c_tier2/c3/RESULTS.md` and `outputs/phase_c_tier2/c3/{narrative, declarative, general}_moral.json` (per-layer fragility for all three conditions).

5 Discussion

5.1 Semantic vs. structural learning dynamics

The Section 4.1 four-curve overlay (Figure 1) shows two distinct learning regimes within a single training run on a single model. The standard moral and sentiment probes, both single-token-swap minimal-pair tasks, emerge as sharp, step-like sigmoidal transitions: each crosses from chance to its plateau within a single 1K-step interval at onset, then flattens. (At 1K sampling we resolve transitions that are step-like at this resolution; we do not claim true discontinuity.) The compositional moral and syntax probes, both tasks that require multi-token integration to determine the label, rise more gradually, with no equally sharp inflection point.

The cleanest hypothesis to organize this dichotomy: **phase-transition dynamics emerge when a feature can be acquired through local lexical or distributional statistics (the model “discovers” the feature in a discrete jump as soon as it has enough samples to distinguish the relevant lexemes), while gradual emergence indicates features that require integrating positional, attentional, or compositional relationships across multiple tokens, which the model cannot acquire in a single step from local lexical statistics alone.** Under this reading the standard moral probe (single-lexeme swap), sentiment (single-adjective swap), and similar lexically-localized tasks all share the phase-transition mechanism; the compositional probe (multi-token integrated swap) and syntax (positional well-formedness) share the gradual-emergence mechanism. The 0.20 plateau gap (Section 4.1) between the two regimes (single-token-statistics tasks saturating near 0.97, multi-token-integration tasks near 0.77) is consistent with this reading: features that can be cleanly read off single-token distributional statistics in mean-pooled hidden states should reach higher linear separability than features that require recovering multi-token interactions from a pooling operation that discards positional information.

The dichotomy connects to Power et al.’s (2022) grokking literature (sudden phase transitions on algorithmic tasks), which has largely focused on the *cause* of phase transitions; our results suggest the *taxonomy* of which capabilities should and should not exhibit them. The formal information-theoretic argument is its own paper.

5.2 Why fragility succeeds where accuracy saturates

Probing accuracy is a thresholded, capped, top-end metric: once linear separability is good enough, accuracy hits ceiling and stops returning information about underlying representational change. Fragility is structurally different: it is sensitive to both the *margin* of separability (outputs near the decision boundary flip under small noise) and the *redundancy* of representation (features encoded in many hidden-space directions tolerate noise that collapses any one). It does not separately identify their contributions, and a low critical noise can also reflect activation-scale changes, representational anisotropy, or probe-training instability rather than margin or redundancy alone. Both margin and redundancy continue to evolve after accuracy saturates because both are functionals of representation *geometry* rather than end-to-end classification accuracy. Concretely (Section 4.2): the standard moral probe’s mean accuracy holds at ~ 0.95 from step 4K through step 36K while early-layer critical noise drops $10.0 \rightarrow 1.8$. The argument generalizes: fragility is not a moral-domain-specific contribution but a methodological contribution for any binary probing task that hits accuracy ceiling.

5.3 Limitations

Lexical \rightarrow compositional gradient bounds the standard probe. The standard moral probe measures something closer to “moralized vocabulary becomes linearly separable from neutral vocabulary” than “moral reasoning emerges.” The compositional probe (Section 4.1) established this is a quantitative gradient: lexically-marked moralized vocabulary at step 1K, compositional moral integration at step 5K, syntactic competence at step 6K, not a binary in-or-out distinction. Both onsets are real findings. Neither of them is “moral reasoning at step 1K”; both are bounded claims about what a linear probe can recover from mean-pooled hidden states at each step.

Compositional probe partial scope. The compositional probe addresses *whether the moral signal lives in single-token vs. multi-token features*; it does not address *whether the model represents moral concepts in any deeper functional sense*: counterfactual sensitivity to moral reframing, generalization to novel moral structures not in pre-training data, behavioral consistency under adversarial probing. The compositional probe is a strictly stronger lexical-accessibility ablation than the standard probe; it is not a moral-reasoning probe. Stronger probes for deeper moral capacities are out of scope for this paper.

Two related questions disambiguate at scale (7B / 32B replication). First, the Section 4.1 plateau coincidence (compositional \approx syntax \approx 0.77 vs. standard moral / sentiment \approx 0.97) may reflect a 1B-model ceiling on compositional / structural encoding or a probe-side ceiling under mean-pooled linear probing. Second, the Section 4.2 4-seed compositional fragility decline through steps 7K-30K (4.65 \rightarrow 2.46), opposite to the standard probe’s late-training hold, admits both a *mechanism reading* (compositional representations drift toward brittleness as training continues on text that does not specifically reinforce them) and a *probe-ceiling reading* (fragility at the 0.77 operating point has less headroom than at 0.96, partly artifacting the difference). Both readings predict different scaling behavior: under the mechanism reading the decline tracks training-text distribution rather than scale, under the probe-ceiling reading it attenuates as scale lifts the operating point. Repeating Section 4.1 and Section 4.2 at 7B and 32B disambiguates both. Either outcome refines the gradient finding without overturning it.

Single model family. All findings are on OLMo-2 1B and OLMo-3 7B. Generalization to other architectures and training recipes is open.

Single language. All probing datasets are English; pretraining data for both target models is dominantly English. Cross-lingual generalization of both the gradient finding and the fragility-resolves-what-accuracy-misses pattern is open.

Raw- σ fragility and what would limit it. We add Gaussian noise in raw activation units (Section 3.4). Hidden-state norms vary across layers and checkpoints, so cross-layer and cross-checkpoint critical-noise comparisons may partly reflect activation-scale drift rather than representational robustness alone. We report raw σ because every comparison we draw uses the same probe and activation cache within a single (layer, checkpoint) cell, which holds the scale fixed; a σ -normalized-by-per-layer-activation-RMS variant is future work. More generally, the fragility finding would be undercut if the layer-depth gradient (Section 4.2) or the declarative-vs-natural separation (Section 4.3) vanished under RMS-normalized noise, or if it tracked activation norm rather than probe margin; we have not yet run that control.

Foundation-specific scope. The standard moral dataset’s six MFT foundations show staggered emergence; all six stabilize by step 3K (Appendix A). The emergence ordering is sensitive to dataset construction choices, which confirms the importance of dataset quality methodology in probing studies; findings that depend on specific pairs rather than the property of interest are artifacts, not discoveries. The compositional dataset’s 200 pairs are categorized by construction pattern (motive / target / consequence / role) rather than by MFT foundation; a foundation-stratified compositional probe (parallel to the foundation-specific standard probe in Appendix A) would tell us whether different foundations acquire compositional encoding at different steps. Out of scope for this paper but a natural extension.

6 Conclusion

Probing accuracy is the wrong instrument for studying training dynamics. Whatever continued representational change a language model undergoes during pre-training after a property becomes linearly decodable (and Section 4 shows there is a great deal of such change) does not register on a metric that has already saturated. The methodological contribution of this paper is to take this saturation as a fixed feature of probing accuracy and add a complementary metric (per-layer critical noise, which we call *fragility*) that recovers the missing resolution. The contribution is not specific to moral representations or to pre-training trajectories; we have established the fragility-resolves-what-accuracy-misses pattern on the standard moral probe (Section 4.2) and on the compositional moral probe across four random- seed splits (Section 4.2, replication). We expect the methodology to extend to any binary probing-based investigation of neural network representations where the operating point is high enough to saturate the standard accuracy curve.

The science findings earn the methodology its keep. The most consequential of them is the *quantitative gradient* the paper establishes by adding the compositional moral probe alongside the standard moral, sentiment, and syntax probes: lexically-marked moralized vocabulary is decoded at step 1K, compositional moral integration at step 5K, syntactic competence at step 6K. The strongest one-sentence summary of the moral probe’s step-1K onset, that “moral encoding emerges within the first 5% of pre-training;” overstates what the standard probe recovers; the gradient framing (“lexically-marked moralized vocabulary at 1K, compositional moral integration at 5K, syntactic competence at 6K”) is the honest reading. We treat this as an existence proof that probing-claims about pre-training emergence should default to lexical-accessibility hedges until a compositional-or-stronger ablation is run.

Two open questions remain. First, does the compositional plateau at ≈ 0.77 lift with model scale (7B / 32B replication of Section 4.1)? The plateau coincidence is a probe-side property at 1B; scale disambiguates whether the ceiling is the model or the instrument. Second, does the fragility-resolves-what-accuracy- misses pattern extend beyond the probing investigations we have run (foundation-stratified compositional probing, counterfactual- sensitivity probing, linguistic-property probes, factual-recall probes, persona-feature probes)? If fragility resolves dynamics that accuracy misses across this broader set, the methodology is a general-purpose tool for alignment-during-pre-training research; if not, the conditions under which it generalizes are themselves the contribution of follow-up work.

The pre-training window does more work than the standard interpretability instrument shows. Adding a fragility readout recovers a substantial fraction of that work. The lexical \rightarrow compositional gradient is what we recover when we apply the methodology to moral representations specifically; the broader claim is that the same methodology will recover analogous structure wherever probing-based investigations of pre-training currently hit the accuracy ceiling.

Acknowledgments and Disclosure of Funding

This work made extensive use of Anthropic’s Claude (the Claude Code agent on Opus 4.6, 4.7, and 4.8) for code scaffolding, experimental scripts, and prose drafting. The author retains responsibility for experimental design, all scientific claims, and final wording.

References

- Guillaume Alain and Yoshua Bengio. Understanding intermediate layers using linear classifier probes. *arXiv preprint arXiv:1610.01644*, 2017. URL <https://arxiv.org/abs/1610.01644>.
- Andy Arditi, Oscar Obeso, Aaquib Syed, Daniel Paleka, Nina Panickssery, Wes Gurnee, and Neel Nanda. Refusal in language models is mediated by a single direction. *arXiv preprint arXiv:2406.11717*, 2024. URL <https://arxiv.org/abs/2406.11717>.
- Yonatan Belinkov. Probing classifiers: Promises, shortcomings, and advances. *Computational Linguistics*, 48(1):207–219, 2022. doi: 10.1162/coli_a_00422.
- Stella Biderman, Hailey Schoelkopf, Quentin Anthony, Herbie Bradley, Kyle O’Brien, Eric Hallahan, Mohammad Aflah Khan, Shivanshu Purohit, USVSN Sai Prashanth, Edward Raff, et al. Pythia: A suite for analyzing large language models across training and scaling. In *International Conference on Machine Learning (ICML)*, 2023. URL <https://arxiv.org/abs/2304.01373>.
- Hendrik Borras, Bernhard Klein, and Holger Fröning. Walking noise: On layer-specific robustness of neural architectures against noisy computations and associated characteristic learning dynamics. *arXiv preprint arXiv:2212.10430*, 2022. URL <https://arxiv.org/abs/2212.10430>.
- Jesse Graham, Jonathan Haidt, Sena Koleva, Matt Motyl, Ravi Iyer, Sean P. Wojcik, and Peter H. Ditto. Moral foundations theory: The pragmatic validity of moral pluralism. *Advances in Experimental Social Psychology*, 47:55–130, 2013. doi: 10.1016/B978-0-12-407236-7.00002-4.
- Dirk Groeneveld, Iz Beltagy, Pete Walsh, Akshita Bhagia, Rodney Kinney, Oyvind Tafjord, et al. OLMo: Accelerating the science of language models. *arXiv preprint arXiv:2402.00838*, 2024. URL <https://arxiv.org/abs/2402.00838>.

- Jonathan Haidt. *The Righteous Mind: Why Good People Are Divided by Politics and Religion*. Vintage Books, 2012.
- John Hewitt and Percy Liang. Designing and interpreting probes with control tasks. In *Proceedings of the 2019 Conference on Empirical Methods in Natural Language Processing and the 9th International Joint Conference on Natural Language Processing (EMNLP-IJCNLP)*, pages 2733–2743, 2019. doi: 10.18653/v1/D19-1275. URL <https://arxiv.org/abs/1909.03368>.
- Edward J. Hu, Yelong Shen, Phillip Wallis, Zeyuan Allen-Zhu, Yuanzhi Li, Shean Wang, Lu Wang, and Weizhu Chen. LoRA: Low-rank adaptation of large language models. In *International Conference on Learning Representations (ICLR)*, 2022. URL <https://arxiv.org/abs/2106.09685>.
- Kevin Meng, David Bau, Alex Andonian, and Yonatan Belinkov. Locating and editing factual associations in GPT. In *Advances in Neural Information Processing Systems (NeurIPS)*, volume 35, 2022. URL <https://arxiv.org/abs/2202.05262>.
- Neel Nanda, Lawrence Chan, Tom Lieberum, Jess Smith, and Jacob Steinhardt. Progress measures for grokking via mechanistic interpretability. In *International Conference on Learning Representations (ICLR)*, 2023. URL <https://arxiv.org/abs/2301.05217>.
- OLMo Team. 2 OLMo 2 furious. *arXiv preprint arXiv:2501.00656*, 2025. URL <https://arxiv.org/abs/2501.00656>.
- Catherine Olsson, Nelson Elhage, Neel Nanda, Nicholas Joseph, Nova DasSarma, Tom Henighan, Ben Mann, Amanda Askell, Yuntao Bai, Anna Chen, et al. In-context learning and induction heads. *Transformer Circuits Thread*, 2022. URL <https://transformer-circuits.pub/2022/in-context-learning-and-induction-heads/index.html>.
- Tiago Pimentel, Josef Valvoda, Rowan Hall Maudslay, Ran Zmigrod, Adina Williams, and Ryan Cotterell. Information-theoretic probing for linguistic structure. In *Proceedings of the 58th Annual Meeting of the Association for Computational Linguistics (ACL)*, 2020. URL <https://arxiv.org/abs/2004.03061>.
- Alethea Power, Yuri Burda, Harri Edwards, Igor Babuschkin, and Vedant Misra. Grokking: Generalization beyond overfitting on small algorithmic datasets. *arXiv preprint arXiv:2201.02177*, 2022. URL <https://arxiv.org/abs/2201.02177>.
- Chen Qian, Jie Zhang, Wei Yao, Dongrui Liu, Zhenfei Yin, Yu Qiao, Yong Liu, and Jing Shao. Towards tracing trustworthiness dynamics: Revisiting pre-training period of large language models. In *Findings of the Association for Computational Linguistics (ACL)*, 2024. URL <https://arxiv.org/abs/2402.19465>.
- Tao Ren, Xiaoyu Luo, and Qiongxiu Li. APEX: Probing neural networks via activation perturbation. *arXiv preprint arXiv:2602.03586*, 2026. URL <https://arxiv.org/abs/2602.03586>.
- Elena Voita and Ivan Titov. Information-theoretic probing with minimum description length. In *Proceedings of the 2020 Conference on Empirical Methods in Natural Language Processing (EMNLP)*, 2020. URL <https://arxiv.org/abs/2003.12298>.
- Andy Zou, Long Phan, Sarah Chen, James Campbell, Phillip Guo, Richard Ren, Alexander Pan, Xuwang Yin, Mantas Mazeika, et al. Representation engineering: A top-down approach to AI transparency. *arXiv preprint arXiv:2310.01405*, 2023. URL <https://arxiv.org/abs/2310.01405>.

Appendices

Supplementary material. Sections referenced from the main paper as “Appendix A”–“Appendix E”.

A Foundation emergence

The standard moral probe’s 240 minimal-pair dataset is balanced across the six Moral Foundations Theory categories (Graham et al., 2013, Haidt, 2012) at 40 pairs per foundation: care/harm, fairness/cheating, loyalty/betrayal, authority/subversion, sanctity/degradation, and liberty/oppression. The foundation- stratified probe (FoundationSpecificProbe) trains a separate linear classifier per foundation, allowing per-foundation onset and plateau analysis across the same 37 OLMo-2 1B early-training checkpoints used in Section 4.

Headline finding. Foundations emerge in a staggered sequence, with all six foundations saturating within the same window where the aggregated standard moral probe onsets. Authority emerges fastest (step 1K); care and fairness follow (step 2K); loyalty, sanctity, and liberty reach 100% by step 3K.

Foundation	Step 0	Step 1K	Step 2K	Step 3K	Step 6K	First step at 100%
authority/subversion	68.8%	100%	100%	100%	100%	1K
care/harm	68.8%	87.5%	100%	93.8%	100%	2K
fairness/cheating	75.0%	75.0%	100%	100%	100%	2K
sanctity/degradation	68.8%	75.0%	93.8%	100%	100%	3K
loyalty/betrayal	62.5%	62.5%	93.8%	100%	100%	3K
liberty/oppression	68.8%	93.8%	87.5%	100%	100%	3K

Per-foundation peak probing accuracy at key OLMo-2 1B early-training checkpoints. Numbers source: outputs/phase_c1/ foundation-specific probe results.

All six foundations stabilize by step 3K. During development, an earlier dataset with weaker neutral-pair quality produced unstable liberty/oppression encoding; the instability resolved when neutral sentences that inadvertently carried moral content were removed. This sensitivity to dataset quality confirms the importance of the validation methodology described in Section 3.1. Authority/subversion emerges fastest (step 1K), followed by care/harm and fairness/cheating (step 2K), with the remaining three foundations reaching 100% at step 3K.

Numbers source: outputs/phase_c1/ (1B trajectory) and outputs/phase_b/b3_foundation_emergence.png (7B comparison).

B Causal-probing divergence

The Section 3 methodology distinguishes *probing accuracy* (how linearly decodable a property is from a layer’s hidden states) from *causal contribution* (how strongly intervening on a layer’s hidden states changes the model’s downstream behavior on the property). The two are conceptually separate (the layer where information is *stored* may be different from the layer where information is *used*), but the distinction is rarely operationalized in moral-representation work, which typically reports probing accuracy and stops there.

We applied the MoralCausalTracer benchmark (an adaptation of Meng et al.’s 2022 ROME causal-tracing methodology to the moral domain) on three OLMo-3 7B checkpoints (early, mid, final) using the same 240-pair standard moral dataset as the probing analysis. The headline finding:

Checkpoint	Peak causal layer	Peak probing layer	Mean indirect effect
Step 0	5	0	0.01

Checkpoint	Peak causal layer	Peak probing layer	Mean indirect effect
Step 705K	5	19	7.84
Step 1,414K	0	10	7.95

Numbers source: *outputs/phase_b/ causal tracer and layer probe results*.

Causal effect magnitude grows substantially over training (mean indirect effect 0.01 \rightarrow 7.95), and the peak causal layer migrates from layer 5 \rightarrow layer 5 \rightarrow layer 0. But the peak probing layer migrates from layer 0 \rightarrow layer 19 \rightarrow layer 10 over the same training. At the final checkpoint, the gap between the layer that most-strongly *encodes* moral information (layer 10) and the layer that most-strongly *influences* downstream moral-relevant generation (layer 0) is 10 layers; the two metrics identify opposite ends of the network.

This is consistent with a “storage vs. use” picture of moral representation in transformer language models: moral information is *stored* in mid-network layers (where probing recovers it cleanly) and *used* in early layers (where intervening on it most-strongly moves the model’s downstream output). The two facts are representational properties of the same model that probing alone cannot recover.

This appendix serves as supporting evidence for the Section 5.2 fragility-as-richer-functional argument: probing accuracy is one functional of the representation geometry; causal contribution is another; fragility is a third. All three keep evolving through training, often in different directions, and a complete picture of how a representation evolves needs all three. We do not develop the storage-vs-use finding as a body contribution because (a) it is not specific to moral representation and (b) it has its own methodological complications (causal-tracing sensitivity to intervention magnitude, choice of decoder probe) that warrant their own paper.

C Standard moral probe validity controls

Three controls are standard for linear-probing studies that claim to measure something beyond surface vocabulary:

1. **Leave-lexeme-out splits.** Train the probe with all pairs containing a target lexeme (e.g. all “betray” pairs) held out; evaluate on those held-out pairs. Test whether probe accuracy transfers to the held-out lexeme set or whether it has memorized per-lexeme decision boundaries.
2. **Paraphrase transfer.** Generate paraphrases of test-set pairs that preserve moral content but vary surface form; evaluate the probe trained on the original test-set pairs on the paraphrased versions. Test whether the probe recovers the moral signal under surface variation or whether it is reading per-pair surface features.
3. **Adversarial lexical swap.** Construct adversarial pairs where a surface feature the probe might be using (sentence length, position of the moral lexeme, presence of specific function words) is decoupled from the moral label. Test whether the probe accuracy degrades on the adversarial set.

The compositional moral probe (Section 3.2) addresses the strongest version of the “your probe is just reading moralized vocabulary” concern *by construction*: pairs share the morally-loaded action verb between halves and differ only in tokens that carry limited moral signal in isolation (unigram lexical floor 0.63). The probe’s compositional encoding is established directly by leave-construction-out transfer (0.85 hidden-state vs. 0.60 bag-of-words) and by decoding 0.20-0.28 above the per-construction lexical floor (Section 3.2, Section 4.1). The compositional probe is a strictly stronger version of the leave-lexeme-out and adversarial-lexical-swap controls combined. Running these three controls on existing checkpoints takes ~4-6 hours of additional MPS time; results will be included in the submission version.

D Compositional probe pair list and per-category breakdown

The 200-pair compositional moral minimal-pair dataset constructed for Section 3.2 and Section 4.1 is released in `deepsteer/datasets/compositional_moral_pairs.py` as the `COMPOSITIONAL_`

MORAL_PAIRS constant. Each pair is a (moral_text, immoral_text) tuple; the file is plain Python with inline comments grouping pairs by category.

D.1 Per-category structure

Index range	Category	Count	Contrast pattern
0-49	action_motive	50	same action verb, motive differs
50-99	action_target	50	same action, target descriptor differs
100-149	action_consequence	50	same action, consequence framing differs
150-199	role_reversal	50	same components, role/target/context determines valence

D.2 Per-category content-only TF-IDF baseline

Pair-disjoint five-fold GroupKFold (each minimal pair held together so its shared skeleton cannot leak across the train / test split), TfidfVectorizer and LogisticRegression(max_iter=1000), scored orientation-invariantly as $\max(\text{acc}, 1 - \text{acc})$:

Category	TF-IDF separability (pair-disjoint)
action_motive	0.64
action_target	0.59
action_consequence	0.61
role_reversal	0.57
Overall (min_df=2)	0.63

These are the *lexical floor*: the bag-of-words separability that the hidden-state transfer-and-lift analysis (Section 3.2, Section 4.1) is measured against, not a stand-alone compositionality certificate. A single-contrast-token minimal pair is lexically separable by construction, so a low floor is neither expected nor required; what establishes compositional encoding is that hidden-state probes transfer across construction categories (0.85 vs. 0.60 bag-of-words) and decode well above these per-construction floors. Pair-disjoint folds and orientation-invariant scoring both matter: random folds leak the shared pair skeleton, and scoring a leaky anti-correlated classifier by raw accuracy understates separability. Numbers source: `deepsteer.datasets.compositional_moral_pairs.content_separability_baseline`.

D.3 Construction-gate verification

`validate_compositional_dataset()` enforces five gates simultaneously and all 200 pairs pass all five:

1. **Length difference** ≤ 2 alphabetic tokens per pair (max observed: 2)
2. **Length band** 8-20 alphabetic tokens per half (range observed: 8-19)
3. **Content-word overlap** ≥ 0.60 (stopwords removed; matches `deepsteer.datasets.validation.validate_pairs` metric)
4. **Strong-valence blacklist**: zero tokens from a 47-word blacklist (murder, torture, stole, assault, etc.) on either side
5. **No exact duplicates** of either side across the 200 pairs

The construction iterated through approximately five rewriting passes to satisfy gate 3 (content-word overlap ≥ 0.60) alongside the multi-word compositional contrast requirement. The two constraints are in genuine tension: compositional contrasts naturally require swapping multiple content words, while ≥ 0.60 content overlap forces single- or two-word swaps within otherwise-identical structure, and the published dataset reflects the achievable balance.

D.4 Representative samples per category

Eight representative pairs (two per category):

action_motive: - *moral*: “She lied to her parents to **protect** her younger brother today” - *immoral*: “She lied to her parents to **humiliate** her younger brother today” - *moral*: “He invited the new colleague to lunch to make her feel **welcome**” - *immoral*: “He invited the new colleague to lunch to make her feel **unwelcome**”

action_target: - *moral*: “He gave the last loaf of bread to the **hungry** stranger at the door” - *immoral*: “He gave the last loaf of bread to the **wealthy** stranger at the door” - *moral*: “She offered her warm coat to the **shivering child** waiting in the rain” - *immoral*: “She offered her warm coat to the **bored heir** waiting in the rain”

action_consequence: - *moral*: “He kept the secret about the surprise to keep his sister **safe** today” - *immoral*: “He kept the secret about the surprise to keep his sister **hurt** today” - *moral*: “She held onto the savings to **provide for her children’s** future education” - *immoral*: “She held onto the savings to **deprive her children of any** future education”

role_reversal: - *moral*: “The judge accepted the gift to free the **innocent** prisoner from prison” - *immoral*: “The judge accepted the gift to free the **guilty** prisoner from prison” - *moral*: “The senator added the amendment to **protect** the whistleblowers from retaliation” - *immoral*: “The senator added the amendment to **expose** the whistleblowers to legal retaliation”

D.5 Full pair list

The complete 200-pair list is released in `deepsteer/datasets/compositional_moral_pairs.py`. The dataset is deterministic and API-free; reproducing the results in Section 4.1 requires only loading the constant and the `LayerWiseMoralProbe / MoralFragilityTest` infrastructure released with the paper.

A camera-ready version of this appendix will inline the full pair list (one pair per row in a table) for archival completeness if the venue’s appendix length allows; otherwise the published code repository is the canonical pair-list reference and this appendix points to it.

The full pair list is available in the released code repository; a camera-ready version of this appendix will inline it if the venue’s appendix length budget allows.

E Reproducibility

E.1 Hardware

All experiments run on a single MacBook Pro M4 Pro: - 12-core CPU (8 performance + 4 efficiency) - 24 GB unified memory (CPU and GPU share) - M4 Pro GPU accessed via PyTorch MPS backend - macOS 25.1.0 (Darwin)

No discrete GPU, no CUDA, no cluster compute. The full Section 4 experimental record ($37 \times 1\text{B}$ early-training checkpoints + $20 \times 7\text{B}$ stage-1 checkpoints + $1 \times 1\text{B}$ final + 4-seed compositional probe + fragility on $37 \times 1\text{B}$ checkpoints + C3 LoRA on 1B at step 1K) totals approximately 6 hours of MPS time across all phases. The dense 1B trajectory + 4-seed compositional fragility replication that produces the paper’s headline numbers fits in ~80 minutes.

E.2 Random seeds

Experiment	Seed(s)	Where set
Standard moral train/test split	42	<code>deepsteer.datasets.pipeline.build_probing_dataset</code>
Sentiment train/test split	42	<code>deepsteer.datasets.sentiment_pairs.get_sentiment_dataset</code>

Experiment	Seed(s)	Where set
Syntax train/test split	42	<code>deepsteer.datasets.syntax_pairs.get_syntax_dataset</code>
Compositional moral train/test split (headline)	42	<code>deepsteer.datasets.compositional_moral_pairs.get_compositional_moral_dataset</code>
Compositional moral 3-seed replication	43, 44, 45	<code>papers/1_accuracy_vs_fragility/scripts/phase_c4_3seed.py</code>
Probe initialization (per-seed)	inherits from split seed via <code>torch.manual_seed(split_seed)</code>	<code>papers/1_accuracy_vs_fragility/scripts/phase_c4_3seed.py</code> line 117, 124
Probe initialization (headline / non-3-seed runs)	unset (system entropy)	—

The original compositional trajectory (split seed 42) and the Section 4.3 LoRA experiment do not set torch’s RNG state explicitly; per-seed reproducibility for those runs is bounded by torch’s deterministic pre-hook RNG state at process start. The 3-seed compositional fragility replication does set `torch.manual_seed(split_seed)` before each per-seed run; per-seed reproducibility for that experiment is exact modulo MPS non-determinism. Seed-to-seed variance in the 3-seed replication therefore reflects both train/test split variation and probe-init variation, which is the relevant quantity for the Section 4.2 decision rule (variance of the probe accuracy as a whole, not just split variance).

E.3 Software versions

- Python 3.13
- PyTorch (with MPS backend)
- HuggingFace transformers
- HuggingFace datasets
- scikit-learn 1.8 (TF-IDF baseline)
- peft (LoRA fine-tuning for Section 4.3)

Exact versions are pinned in `pyproject.toml` in the released codebase; we use the repo’s standard environment without any experiment-specific dependency overrides.

Public release. All code, datasets, scripts, and per-checkpoint output JSON are released at <https://github.com/deepsteer/deepsteer/>; the paper-specific subdirectory (this paper’s section sources, build pipeline, generation scripts, and outputs) is at https://github.com/deepsteer/deepsteer/tree/main/papers/1_accuracy_vs_fragility.

E.4 Model checkpoints

All target models are HuggingFace repos under the allenai organization:

Model	Repo	Used for
OLMo-2 1B early-training	<code>allenai/OLMo-2-0425-1B-early-training</code>	Section 4.1 trajectory, Section 4.2 fragility, Section 4.3 C3 base
OLMo-2 1B final (~2.2T tokens)	<code>allenai/OLMo-2-0425-1B</code>	Section 3.2 / Section 4.1 compositional probe validation gate
OLMo-3 7B stage-1	<code>allenai/OLMo-3-7B</code> (revisions, see codebase)	Section 4.2 7B fragility corroboration, Appendix B causal tracing

Specific checkpoint revisions for each step are listed in `papers/1_accuracy_vs_fragility/outputs/phase_c1/phase_c1_plan.json` (1B trajectory), `papers/1_accuracy_vs_`

fragility/outputs/phase_c4_compositional/compositional_per_checkpoint.json (1B compositional probe), and papers/1_accuracy_vs_fragility/outputs/phase_b/phase_b_plan.json (7B trajectory).

E.5 Command-line invocations to reproduce each result

All commands run from the project root.

```
# §4.1 standard moral / sentiment / syntax onsets (Phase C2)
python papers/1_accuracy_vs_fragility/scripts/c2_linguistic_comparison.py

# §4.1 compositional moral onset (Phase C4 trajectory + validation)
python papers/1_accuracy_vs_fragility/scripts/phase_c4_compositional.py

# §4.2 standard moral fragility evolution (Phase C1)
python papers/1_accuracy_vs_fragility/scripts/phase_c1.py

# §4.2 4-seed compositional fragility replication
python papers/1_accuracy_vs_fragility/scripts/phase_c4_3seed.py

# §4.3 C3 LoRA narrative vs. declarative vs. control
python papers/1_accuracy_vs_fragility/scripts/phase_c_tier2.py --condition narrative_moral
python papers/1_accuracy_vs_fragility/scripts/phase_c_tier2.py --condition declarative_moral
python papers/1_accuracy_vs_fragility/scripts/phase_c_tier2.py --condition general_control

# §4.1 Figure 1 (4-seed compositional band overlay) --- regenerate
python papers/1_accuracy_vs_fragility/scripts/figure_1_onset_overlay.py
```

Each script is self-contained, reads no environment-specific configuration, and writes structured JSON output to papers/1_accuracy_vs_fragility/outputs/<phase>/ with full metadata (model name, revision, timestamp, hyperparameters, dataset version) per the project’s reproducibility convention. A researcher should be able to reproduce any number reported in the paper from the corresponding output JSON without re-deriving the analysis.

E.6 Output JSON schema

The two output JSON file types load-bearing for Section 4 results:

- `LayerProbingResult` (`deepsteer.core.types.LayerProbingResult`) for probe-trajectory data. Fields: `benchmark_name`, `model_info` (with `name`, `provider`, `access_tier`, `n_layers`, `n_params`, `checkpoint_step`), `layer_scores` (list of per-layer {`layer`, `accuracy`, `loss`}), `onset_layer`, `peak_layer`, `peak_accuracy`, `moral_encoding_depth`, `moral_encoding_breadth`, `metadata`.
- `FragilityResult` (`deepsteer.core.types.FragilityResult`) for fragility-test data. Fields: `benchmark_name`, `model_info`, `layer_scores` (per-layer {`layer`, `baseline_accuracy`, `accuracy_by_noise`, `critical_noise`}), `noise_levels`, `mean_critical_noise`, `most_fragile_layer`, `most_robust_layer`, `metadata`.

The schemas are stable; field names match the dataclass attributes in `deepsteer/core/types.py`. JSON serialization uses `_dataclass_to_dict` (see same file).

E.7 Dataset version

All experiments in this paper use the moral probing dataset (`deepsteer/datasets/moral_probing_v2.json`), loaded via `build_probing_dataset(dataset_version="v2")`. The dataset contains 1,200 minimal pairs (200 per MFT foundation) constructed from quality-audited seed examples (`seed_examples_v3.json`) via a `generate`→`rate`→`assemble` pipeline with LLM-assisted filtering for naturalness (§1.3) and moral neutrality of neutral-side sentences (§1.5). The 240-pair subset used for probing (40 per foundation) is a deterministic seed-42 subsample. Construction methodol-

ogy, quality audit dimensions, and filtering thresholds are documented in DATASET_GUIDELINES.md in the released codebase.

SHA256 checksum of the dataset file used for all results in this paper:

eb052885d5c6f7ed18aaeeb507eb0ce3d6106350e3fb4960d76f2fbd77f129ea moral_probing_v2.json